

Molecular treatment of electron capture in collisions of N^{4+} ions with H atoms

N. Shimakura

General Education Department, Niigata University, Niigata 950-21, Japan

M. Itoh*

Department of Chemistry, Faculty of Science, Niigata University, Niigata 950-21, Japan

M. Kimura

*Argonne National Laboratory, Argonne, Illinois 60439
and Department of Physics, Rice University, Houston, Texas 77251*

(Received 2 July 1991)

Partial and total cross sections of electron-capture processes in collision of N^{4+} ions with H atoms are calculated in the collision energy range from 1 eV/amu to 10 keV/amu. Semiclassical and quantum-mechanical molecular-orbital methods with electron translation factors are employed. Two-electron processes are also considered, but they are found to make small contributions at all collision energies. The dominant electron-capture channels are found to be the $N^{3+}(3p)$ state at energies above 300 eV/amu and the $N^{3+}(3d)$ state at energies lower than 300 eV/amu. Three experiments that observed only total cross sections have been reported for this system. The agreement of the present calculation with these measurements is excellent at all energies. In particular, an oscillation observed in the experiment of Huq, Havener, and Phaneuf [Phys. Rev. A **40**, 1811 (1989)] is reproduced by our calculation in the energy range 10–300 eV, and the origin of the oscillation is discussed.

PACS number(s): 34.10.+x, 34.20.-b, 34.70.+e

I. INTRODUCTION

Electron-capture processes in collisions of multiply charged ions with atoms have been a central focus of research on atomic collisions for the past decades. This trend is due, in part, to applications in other areas of technology and in other subfields of physics [1]. However, most theoretical and experimental studies have been devoted to electron-capture processes within a relatively narrow energy region. In addition, relatively few calculations for the systems have involved two active electrons simultaneously.

In this paper, we present the results of a detailed calculation of the cross sections for electron capture from H by N^{4+} in the energy range from eV/amu to 10 keV/amu. This work is an extension of our previous calculation for the $(N^{5+}+H)$ system [2]. While the $(N^{5+}+H)$ system could be treated as a pseudo-one-electron system, the $(N^{4+}+H)$ system possesses two active electrons. A study of the role of the additional electron or the electron correlation in the collision process is very interesting. Three measurements have been reported for this system, two of them performed at intermediate collision energies of 1–7 keV/amu by Crandall *et al.* [3] and 1.1–3.6 keV/amu by Seim *et al.* [4]. Below 1 keV/amu, Huq *et al.* [5] recently determined the total capture cross sections.

Only one theoretical study, by Feickert *et al.* [6] exists for the system at very low collision energies below 2.5 eV/amu. In their calculations, the authors adopted several assumptions whose validities are certainly questionable for a quantitative discussion of the results. The

method of Feickert *et al.* [6] is as follows: (i) Determine the electronic structure by using the *ab initio* configuration-interaction (CI) method with a Gaussian basis set. Only configurations of one active electron were considered. (ii) Roughly estimate the coupling matrix elements from the obtained potential energies. (iii) Perform a quantum-mechanical close-coupling calculation with inclusion of four Σ states: initial, $N^{3+}(2s3s)+H^+$, $N^{3+}(2s3p)+H^+$, and $N^{3+}(2s3d)+H^+$ channels. As we will show, their treatments (i) and (ii) are less accurate than those in the present treatment.

II. FORMULATION

Since the details of the method employed in this paper have been described previously [2,7] only the brief summary of the basic technique and the specific information used for the calculation are given here.

A. Molecular states

The molecular electronic states are obtained by using a modified valence-bond CI method with Gaussian-type pseudopotentials representing the N^{5+} core [8], which reduces the four-electron system to a two-electron system. Our form of the pseudopotential is

$$V(\mathbf{r}) = \sum_{l,m} V_l(r) |Y_{lm}\rangle \langle Y_{lm}| \quad (1)$$

and

$$V_l(r) = A_l \exp(-\xi_l r^2) - \frac{\alpha_d}{2(r^2 + d^2)^2} - \frac{\alpha_q}{2(r^2 + d^2)^3} + \frac{5}{r}, \quad (2)$$

where $|Y_{lm}\rangle$ are the spherical harmonics. In Eq. (2), A_l and ξ_l are l -dependent parameters chosen to fit asymptotic eigenvalues to spectroscopic data [9]. Values of the dipole and quadrupole polarizabilities α_d and α_q were taken from the review by Dalgarno [10]. The cutoff radius d was determined by a Hartree-Fock calculation. The pseudopotential parameters are given in Table I.

We expand the molecular wave function in terms of Slater determinants. Slater-type orbitals (STO's) used as our basis sets consisted of 38 STO's for N^{4+} and N^{3+} ions and 10 STO's for the H atom. For the triplet system, the orbital exponents for the N^{4+} and N^{3+} ions were obtained by optimizing the energies. For the singlet system, those energies were also optimized separately. However, the singlet orbital exponents gave nearly identical results for energies as values for the triplet manifold do. Hence, the same orbital exponents for both the singlet and triplet systems were used in this calculation. The orbital exponents of the H atom were taken from previous work by Sato *et al.* [11]. The Slater exponents used are given in Table II. The accuracy of the present molecular calculation with respect to the spectroscopic energies [9] is better than 0.5% for all states. As a measure of the accuracy, the calculated values for the asymptotic energy defect, ΔE , of the electron-capture process [$\Delta E = E(N^{4+}(2s) + H) - E(N^{3+}(nl n' l') + H^+)$] are compared with the spectroscopic values [9] and values of Feickert *et al.* [6] in Table III, which clearly shows that our values are in better agreement with the experimental values than with those of Feickert *et al.* Note that, because Feickert *et al.* considered only one electron to be active [6], no state corresponds to two-electron processes such as $N^{3+}(2p3s) + H^+$ and $N^{3+}(2p2p) + H^+$ in their calculation.

B. Collision dynamics

A fully quantum-mechanical and a semiclassical close-coupling method [7] with a molecular-orbital base ob-

TABLE I. N^{5+} core pseudopotential parameters.

Parameter	Value (a.u.)
A_0	54.555 325 339
A_1	-2.703 778 324 36
A_2	-0.472 270 196 513
ξ_0	9.682 625 759 99
ξ_1	10.998 562 837 5
ξ_2	7.014 003 190 62
d	0.227 279 7
α_d	0.004 63
α_q	0.000 38

TABLE II. Orbital exponents of the Slater-type orbital basis function.

N^{4+} and N^{3+}		H	
Orbital	Exponent	Orbital	Exponent
2s	11.876 342	1s	2.0
	4.954 557 6		1.0
	2.791 479 7		0.5
	1.759 458 5	2s	0.5
2p	4.938		1.0
	2.688	2p	0.5
1.589			
3s	1.483 11		
3p	1.637 96		
3d	1.463 82		
4s	1.324 59		
4p	1.150 19		
4d	1.214 42		
4f	1.253 77		

tained in the procedure above have been used below and above 20 eV/amu, respectively. Atomic-type (plane-wave) electron translation factors (ETF's) up to first order in velocity were included in both methods [2,12]. These coupled equations were solved numerically with appropriate boundary conditions.

1. The quantum-mechanical representation

Due to a sharp radial coupling at an avoided crossing region involved, it is numerically more convenient to treat the coupled equation in diabatic representation rather than in original adiabatic representation. The transformation to the diabatic representation can be achieved through a transformation matrix $C(\mathbf{R})$ [13]. In this representation, the coupling matrix is represented by the potential coupling matrix as $V^d = C^{-1} V^a C$, where V^a is the adiabatic potential matrix.

In the diabatic representation, the nuclear wave function \underline{X}^d satisfies

$$\left[\frac{1}{2\mu} \nabla_R^2 I - \underline{V}^d(R) + EI \right] \underline{X}^d(R) = 0, \quad (3)$$

where I is the identity matrix and μ is the reduced mass. Equation (3) is solved numerically for each partial wave by using the log derivative method [14] to extract the scattering S_{ij}^l matrix for the $i \rightarrow j$ transition. From the S_{ij}^l matrix for each partial wave, the total cross section can be easily obtained [7,15].

2. The semiclassical representation

Expanding the total wave function in terms of the molecular wave function and the ETF and substituting the total wave function into the time-dependent Schrödinger equation yields ordinary first-order coupled equations [7,12] with the ETF effect in the first order of v . A straight line and Coulomb trajectories are assumed for

TABLE III. Asymptotic energies of the states which are referenced by $N^{4+}(2s)+H(1s)$, i.e., $\Delta E = E(N^{4+}(2s)+H) - E(N^{3+}(nan'\beta)+H^+)$.

N^{3+} state $nan'\beta$	ΔE		
	Ref. [9]	Ref. [6]	Present
Triplet system			
$2s2p$	2.040 584	2.029 3 (0.011)	2.054 721 (0.014)
$2s3p$	0.628 063	0.6213 (0.006 0)	0.627 289 (0.000 8)
$2s3p$	0.497 284	0.488 3 (0.009 0)	0.498 649 (0.001 4)
$2s3d$	0.433 212	0.423 3 (0.009 9)	0.427 397 (0.0058)
$2p3s$	0.226 713		0.230 702 (0.004 0)
$2p3p$	0.139 122		0.135 987 (0.003 1)
Singlet system			
$2s^2$	2.347 568		2.357 939 (0.010 4)
$2s2p$	1.752 088	1.680 3 (0.071 8)	1.689 699 (0.062 4)
$2p^2$	1.486 93		1.461 422 (0.025 5)
$2p2p'$	1.275 09		1.231 912 (0.043 2)
$2s3s$	0.575 682	0.569 3 (0.006 4)	0.577 492 (0.001 8)
$2s3p$	0.504 286	0.462 3 (0.042 0)	0.501 452 (0.002 8)
$2s3d$	0.392 018	0.384 3 (0.007 7)	0.375 572 (0.016 0)
$2p3s$	0.179 419		0.185 672 (0.006 2)

heavy-particle motion in the present calculation. The square of the scattering amplitude gives a transition probability to a state at a given collision energy and impact parameter (b). Integration of impact-parameter-weighted probabilities over impact parameter yields the total cross sections.

III. RESULTS

A. Adiabatic potential curves

The calculated potential energies for the triplet and singlet systems of the NH^{4+} system are presented in Figs. 1(a) and 1(b), respectively. These figures imply that the $N^{3+}(2s3l)$ states dominate electron capture at low to intermediate energies. Although crossings appear between the 5Σ and 6Σ states at $R = 13.5$ a.u. for the triplet system and between the 7Σ and 8Σ states at $R = 16.0$ a.u. for the singlet system, the corresponding energy splittings are extremely small, with values of 8×10^{-5} and 2×10^{-5} a.u., respectively; hence, these crossings are considered to be near diabatic in the actual collision events.

For the triplet system, an important avoided crossing can be seen at about 7.15 a.u. ($=R_5$) between the 4Σ and 5Σ states with an energy splitting of about 2.0×10^{-2} a.u. in the present results. The corresponding avoided crossing obtained by Feickert *et al.* [6] appears to be at about 7.20 a.u. with energy splitting of about 1.4×10^{-2} a.u. At smaller internuclear distances, three avoided crossings occur at about 3.37 ($=R_1$), 4.19 ($=R_2$), and 4.45 a.u. ($=R_3$), with energy splittings of about 7.5×10^{-3} , 2.0×10^{-4} , and 1.7×10^{-2} a.u., respectively. These crossings, due to our inclusion of the two-electron processes, are completely missing in the calculation of Feickert *et al.* [6]. A broad avoided crossing can be seen at about 6.0 a.u. ($=R_4$) with energy splitting of about 1.1×10^{-1} a.u. We find that the $N^{3+}(2l2l')$ states do not

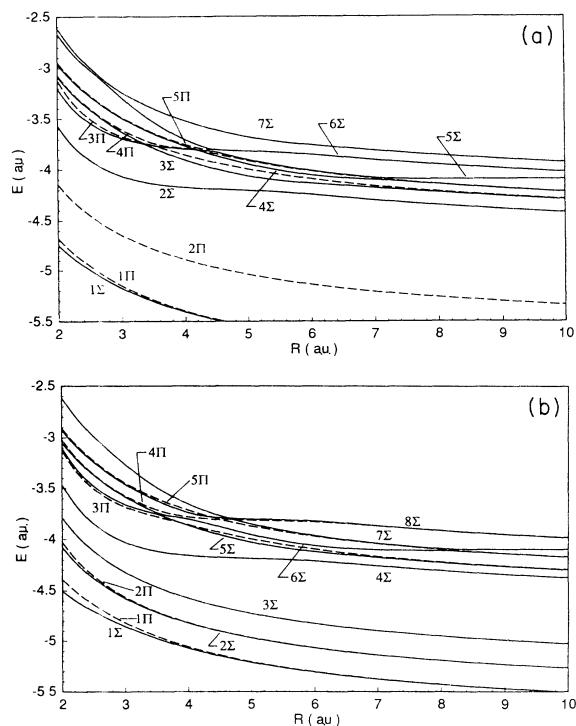


FIG. 1. (a) Adiabatic potentials for the triplet NH^{4+} system. Solid and dashed curves represent Σ and Π states, respectively. 1Σ and 1Π , $N^{3+}(2s2p)+H^+$; 2Π , $N^{3+}(2p2p')+H^+$; 2Σ , $N^{3+}(2s3s)+H^+$; 3Σ and 3Π , $N^{3+}(2s3p)+H^+$; 4Σ and 4Π , $N^{3+}(2s3d)+H^+$; 5Σ , $N^{4+}(2s)+H$; 6Σ and 5Π , $N^{3+}(2p3s)+H^+$; 7Σ , $N^{3+}(2p3p)+H^+$. (b) Adiabatic potentials for the singlet NH^{4+} system. Solid and dashed curves represent Σ and Π states, respectively. 1Σ and 1Π , $N^{3+}(2s2p)+H^+$; 2Σ and 2Π , $N^{3+}(2p2p)+H^+$; 3Σ , $N^{3+}(2s2p')+H^+$; 4Σ , $N^{3+}(2s3s)+H^+$; 5Σ and 3Π , $N^{3+}(2s3p)+H^+$; 6Σ and 4Π , $N^{3+}(2s3d)+H^+$; 7Σ , $N^{4+}(2s)+H$; 8Σ and 5Π , $N^{3+}(2p3s)+H^+$.

significantly contribute to the electron-capture processes except at high collision energies.

For the singlet system, the lowest Σ state [$N^{3+}(2s^2)+H^+$] is not displayed in Fig. 1(b) because it is located far below the initial channel and it plays no role in the electron-capture process. General features of the potential energies for the singlet system are similar to those observed in the triplet system except for the 2Σ and 3Σ states. The avoided crossings appear at about 3.54 ($=R_1$), 4.20 ($=R_2$), 4.65 ($=R_3$), 6.20 ($=R_4$), and 8.15 a.u. ($=R_5$) with energy splittings of about 1.4×10^{-2} , 1.6×10^{-1} , 5.8×10^{-3} , 1.6×10^{-1} , and 1.9×10^{-2} a.u., respectively.

The avoided crossings in the potential energies for the triplet and singlet systems appear at the nearly same internuclear distances except at R_5 . The energy splittings at R_1 and R_4 also have nearly the same values, but the splitting at R_2 in the triplet system is much smaller than that in the singlet system. At R_3 the situation is reversed, but the difference is not as large. As Table III shows, the asymptotic energy defect of the $N^{3+}(2s3d)$ state for the triplet system is larger than that for the singlet system. This phenomenon pushes the location of the avoided crossing between the 4Σ and 5Σ states in the triplet system into smaller R than that between the 6Σ and 7Σ states in the singlet system. Furthermore, it explains why, at internuclear distances of 4.5–6.5 a.u., the difference of the potential energies between the 4Σ and 5Σ states in the triplet system is smaller than that between the 6Σ and 7Σ states in the singlet system. The second point is important in connection with an oscillation appearing in the total cross section for the triplet system (see Sec. III C 1).

B. Coupling matrix elements

The representative results of radial couplings are displayed in Figs. 2(a) and 2(b) for the triplet and the singlet systems, respectively. For the triplet system, the peaks seen at $R = 7.15$, 4.45, and 3.37 a.u. are due to avoided crossings between the 4Σ and 5Σ , the 5Σ and 6Σ , and the 3Σ and 4Σ states, respectively. Note that there is a secondary peak in the coupling between 5Σ and 4Σ at $R = 4.5$ a.u. and this secondary peak plays a crucial role in causing oscillatory structures in the cross section. The coupling between the 4Σ and 5Σ states at R_2 is very large (≈ 400 a.u.) and is very sharp (half-width is 2.8×10^{-3} a.u.) (not shown) and because of these characteristics of the coupling we decided to treat this crossing as diabatic in the close-coupling calculation. For the singlet system, the peaks appearing at $R = 8.15$, 4.65, 4.20, and 3.54 a.u. between the 6Σ and 7Σ , the 7Σ and 8Σ , the 6Σ and 7Σ , and the 5Σ and 6Σ states, respectively, are dominant for the dynamics.

C. Cross sections

For the triplet system, a 12-channel close-coupling calculation was performed to obtain the electron-capture probability in the energy range from 15 eV/amu to 10 keV/amu. In this calculation, all seven Σ states and five Π states, as shown in Fig. 1(a), were included. For the

singlet system, a 13-channel close-coupling calculation was performed, in which all eight Σ states and five Π states, as shown in Fig. 1(b), were included. In this calculation, we did not include the $N^{3+}(2p3p)+H^+$ channel, which was included for the triplet system. We wanted to examine the trajectory effect on the transition probabilities for a wide range of energies by using two kinds of trajectories. For this purpose, we used both straight-line and repulsive Coulomb trajectories for heavy-particle motion.

In the low-energy region, two-state quantum-mechanical close-coupling calculations were performed with the initial and $N^{3+}(2s3d)+H^+$ channel. Our semiclassical calculation showed that, at low collision energies, only the $N^{3+}(2s3d)+H^+$ channel is solely dominant for the electron-capture process. However, at internuclear distances less than R_3 , the transfer-excitation state complicates the treatment of the close-coupling calculation. The two channels used in quantum-mechanical calculations for the triplet system were constituted as follows. The first channel, the 5Σ state at internuclear distances larger than R_3 , is connected smoothly to the 6Σ state at internuclear distances smaller than R_3 . The second channel, the 4Σ state at internuclear distances larger than R_2 , is connected smoothly to the 5Σ state at smaller internuclear distance. For the singlet system, the first channel, the 7Σ state at internuclear distances larger

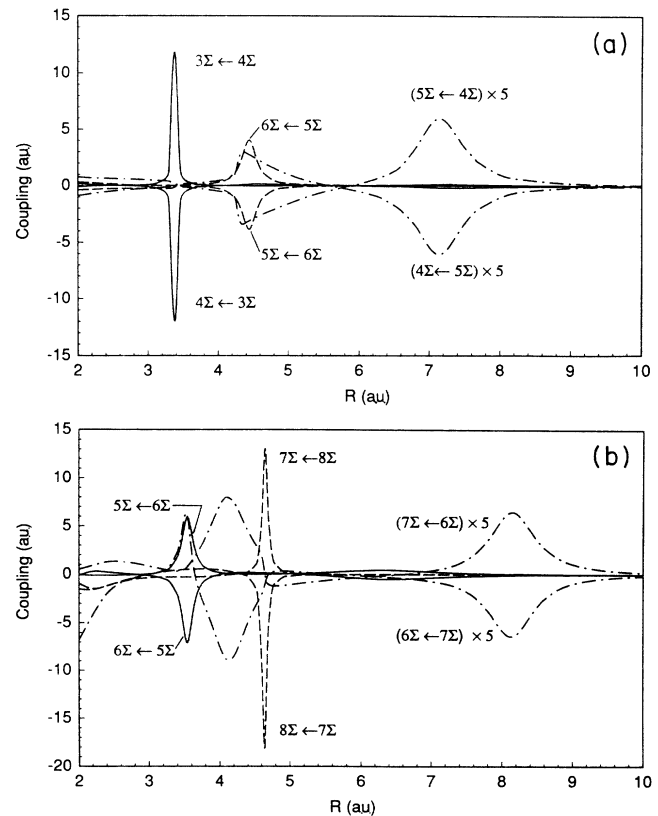


FIG. 2. Calculated representative radial couplings for (a) the triplet and (b) the singlet systems, respectively.

than R_3 , is connected smoothly to the 8Σ state at smaller internuclear distances than R_3 . The second channel, the 6Σ state at the internuclear distances larger than R_1 , is connected smoothly to the 5Σ state at the smaller internuclear distances. In Sec. III D 3, we return to this point.

Figure 3 shows the calculated partial and total cross sections for the triplet system. Solid and dashed curves represent the semiclassical results for straight-line and Coulomb trajectories, respectively. At the collision energy 560 eV/amu, the difference between the cross sections obtained by those two trajectories is only 3.0%, but at 78 eV/amu, the difference increases to 18.0%. A gentle oscillation clearly visible in the total cross sections in the energy range from 15 to 300 eV/amu reflects the structure of the partial cross section for the $N^{3+}(2s3d)$ state. At higher energies, capture into the $N^{3+}(2s3p)$ state is a main contributor, but the $N^{3+}(2s3s)$ and $N^{3+}(2s3d)$ states also contribute to some extent. At low energies, only capture into the $N^{3+}(2s3d)$ state is appreciable. In all energy ranges studied, a small contribution comes from the $N^{3+}(2p3s)$ state; this contribution is not more than 10% of the total cross section. The $N^{3+}(2p3s)$ state corresponds to a two-electron process (i.e., transfer excitation); one electron is transferred, and at the same time another electron is excited. In the low-energy region, the quantum-mechanical results are shown by dash-dotted curves. Their values decrease monotonically as the energy decreases.

As representative examples, the collision histories (i.e., the time evolutions of the transition probabilities) of several dominant states for the triplet system are plotted as a function of internuclear distance (and time) at impact parameter $b = 5.0$ a.u. in cases of $E = 562.5$ and 78.4 eV/amu, in Figs. 4(a) and 4(b), respectively. Under these conditions, the transition probabilities to any state except the $N^{3+}(2s3s)$, $N^{3+}(2s3p)$, $N^{3+}(2s3d)$, and $N^{3+}(2p3s)$ states are negligible. As Fig. 4(a) shows, at high collision energies the transition from the 4Σ [$N^{3+}(2s3d)$] state to the 3Σ [$N^{3+}(2s3p)$] state is very effective after the transition from the 5Σ (initial) state to the 4Σ [$N^{3+}(2s3d)$] state. The transition to the 2Σ [$N^{3+}(2s3s)$] state also

proceeds to some extent. Comparison of Fig. 4(b) with Fig. 4(a) clearly indicates that as collision energy decreases, the transition from the 4Σ state to the 3Σ state decreases. This is because the energy difference between the 4Σ and 3Σ states is rather large. ($\approx 7.3 \times 10^{-2}$ a.u.) and the corresponding radial coupling is rather weak (height ≈ 0.1 a.u.) at the avoided crossing.

The calculated partial and total cross sections for the singlet system are shown in Fig. 5. The overall trend of the cross section is similar to that of the triplet system. However, the oscillation appearing in the triplet system at $E \geq 50$ eV/amu is comparatively suppressed in this case. At all energy ranges, the contribution from the $N^{3+}(2p3s)$ transfer-excitation state is somewhat larger than in the triplet system. The total cross sections are also slightly larger than in the triplet system.

1. Oscillation structure

In the triplet system an oscillation appears in the cross section that is not visible in the singlet system. In this section we discuss the origin of the oscillation structure. Figure 6(a) shows the transition probabilities as a func-

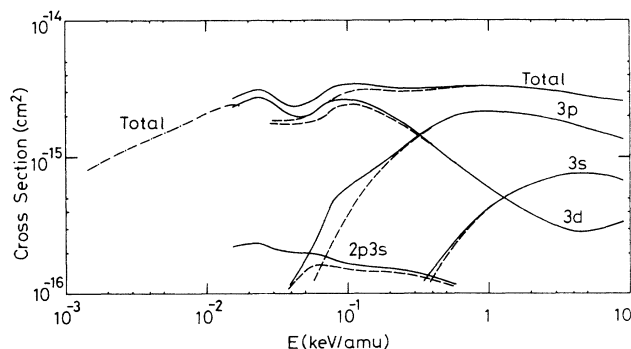


FIG. 3. Collision energy dependence of the total and partial electron-capture cross sections for the triplet system. Solid and dashed curves represent the semiclassical results for straight-line and Coulomb trajectories, respectively. The dash-dotted curve represents the quantum-mechanical results.

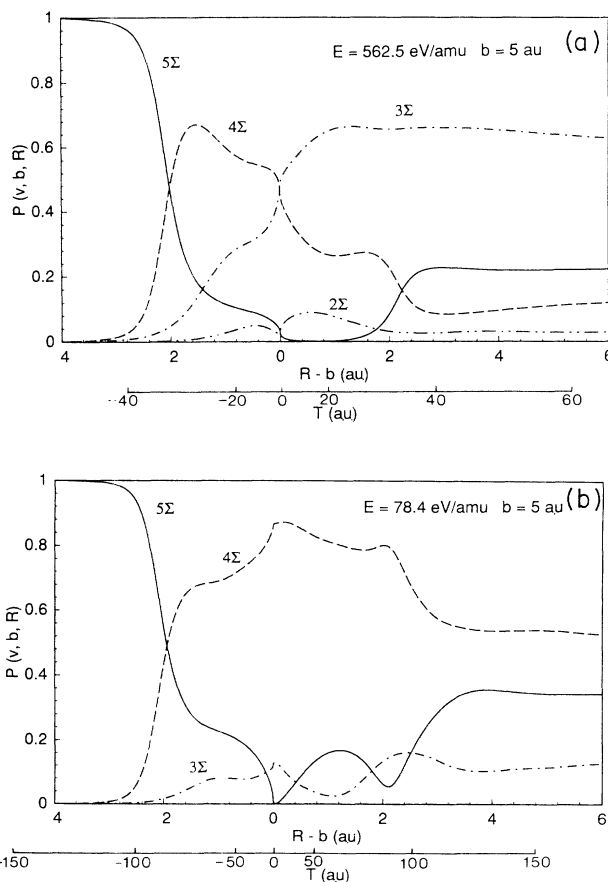


FIG. 4. Collision histories of transition probabilities as a function of R (and time) for (a) $E = 562.5$ eV/amu and (b) $E = 78.4$ eV/amu at $b = 5.0$ a.u.

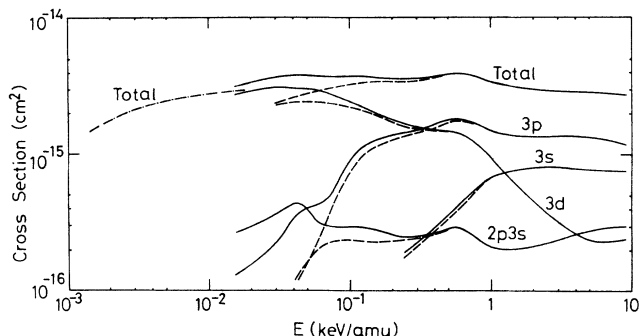


FIG. 5. Collision energy dependence of the total and partial electron-capture cross sections for the singlet system. Solid and dashed curves represent the semiclassical results for straight-line and Coulomb trajectories, respectively. The dash-dotted curve represents the quantum-mechanical results.

tion of the impact parameter for the triplet system at collision energies 30.6, 42.0, 62.5, and 78.4 eV/amu. This figure indicates that in the triplet system all transitions take place at less than $b = 7.0$ a.u. and that, at impact parameters less than 4.0 a.u., an oscillation appears comparatively regularly. However, at impact parameters $b = 4.2$ –6.0 a.u., the transition probabilities show an ir-

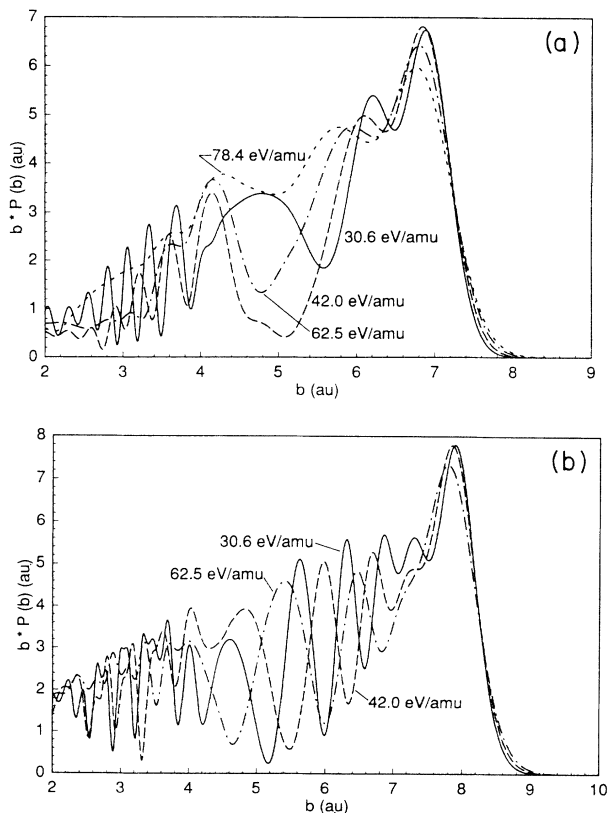


FIG. 6. Total transition probabilities (a) at $E = 30.6, 42.0, 62.5,$ and 78.4 eV/amu for the triplet system and (b) at $E = 30.6, 42.0,$ and 62.5 eV/amu for the singlet system.

regular oscillatory feature. The reason for this characteristic feature is considered to be as follows. In the triplet system, the energy difference between the 4Σ and 5Σ states at $R = 4.5$ –6.0 a.u. is small even though it does not show a clear sign of an avoided crossing like the one at $R = 7.0$ a.u. and the corresponding radial coupling between those states has an additional secondary peak at $R \approx 4.5$ a.u. [as shown in Fig. 2(a)]. Hence, transfer occurs rather effectively at these internuclear separations. This additional transfer dynamics is very sensitive to collision energies in connection with couplings with other states at $R = 4.5$ –6.0 a.u. and this sensitivity can be easily observed in Fig. 6(a). As the collision energy decreases from 78.4 to 42.0 eV/amu, the transition probabilities at $b = 4$ –6 a.u. are drastically reduced while those back up having a broad peak when the collision energy is 30.6 eV/amu.

In Fig. 6(b), the transition probabilities as a function of impact parameter are displayed for the singlet system at collision energies 30.6, 42.0, and 62.5 eV/amu. This figure shows that, in the singlet system, the transition is confined within about $b = 8.0$ a.u. As the impact parameter decreases, an oscillation appears comparatively regularly over all impact parameters. In the singlet system, the energy difference between the 6Σ and 7Σ states at $R = 4.5$ –6.5 a.u. is larger, and the corresponding coupling is smaller than those in the triplet system [as shown in Figs. 2(a) and 2(b)], so transfer is not effective at these internuclear distances. As the collision energy decreases, all peaks shift toward larger impact parameter without drastic change of the general structure. As a result, the total cross sections are smooth as a function of collision energy in the singlet system.

2. Comparison with measurements and another calculation

In Fig. 7, we display the total cross sections from the present work along with measurements [3–5] and another calculation [6]. Our total cross sections are deter-

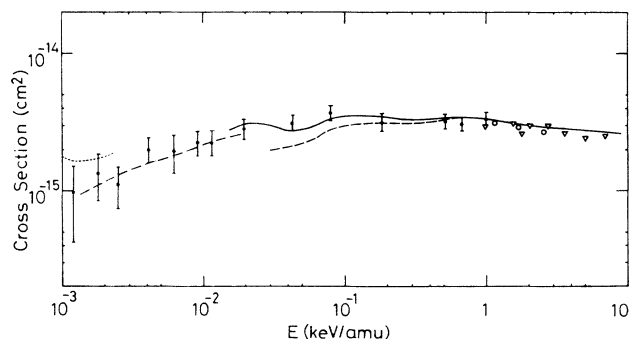


FIG. 7. Collision energy dependence of total electron-capture cross sections. Solid and dashed curves present results obtained by the semiclassical method using straight-line and Coulomb trajectories, respectively. The dash-dotted curve presents results obtained by the quantum-mechanical method. The dotted curve is the calculated results of Feickert *et al.* [6]. Measurements are also shown: ●, Ref. [5]; ▽, Ref. [4]; ○, Ref. [3].

mined by using the values of the triplet and singlet systems with appropriate statistical weights. The calculated results using a straight-line trajectory are in good agreement with all the measurements over the entire energy region studied. The results using a Coulomb trajectory becomes smaller than those using a straight-line trajectory and hence the experiments at low collision energies, as expected. We have reported a similar tendency in the ($N^{5+} + H$) system [2]. The oscillation observed in the experiment is reproduced in our calculation and the origin of the oscillation is interpreted above. The results calculated by Feickert *et al.* [6] are larger than ours and experimental values at 2 eV/amu by approximately a factor of 2 with an increasing trend at lower energies. A qualitative, marked difference also exists between their results and ours; Feickert *et al.* found that the dominant electron-capture channel is the $N^{3+}(2s3d)$ state at the collision energies below about 1.8 eV/amu, but that above this energy it is the $N^{3+}(2s3p)$ state. On the other hand, in our semiclassical calculation, the dominant channel from 15 up to about 300 eV/amu is the $N^{3+}(2s3d)$ state (Figs. 3 and 5). No conclusion about this point can be reached until a more elaborate quantum-mechanical close-coupling calculation is performed.

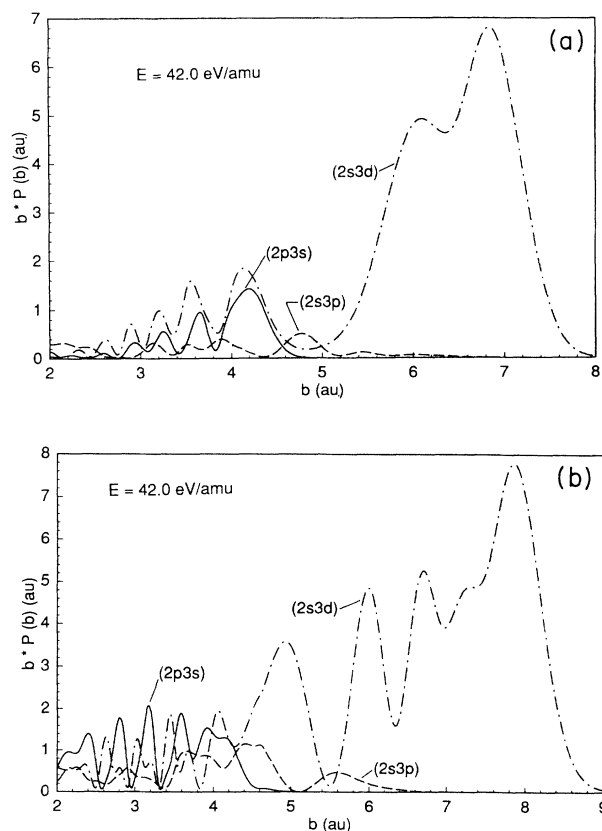


FIG. 8. Partial transition probabilities at $E = 42.0$ eV/amu for the (a) triplet and (b) singlet systems. ($2s3d$), ($2s3p$), and ($2p3s$) represent $N^{3+}(2s3d) + H^+$, $N^{3+}(2s3p) + H^+$, and $N^{3+}(2p3s) + H^+$.

3. Transfer excitation

The transition to the $N^{3+}(2p3s)$ state, corresponding to the transfer-excitation state, is not visible in Figs. 4(a) and 4(b). This is always the case for an impact parameter larger than 4.45 a.u. for the triplet and 4.65 a.u. for the singlet systems at any collision energy. To discuss the transfer-excitation process, we first display the transition

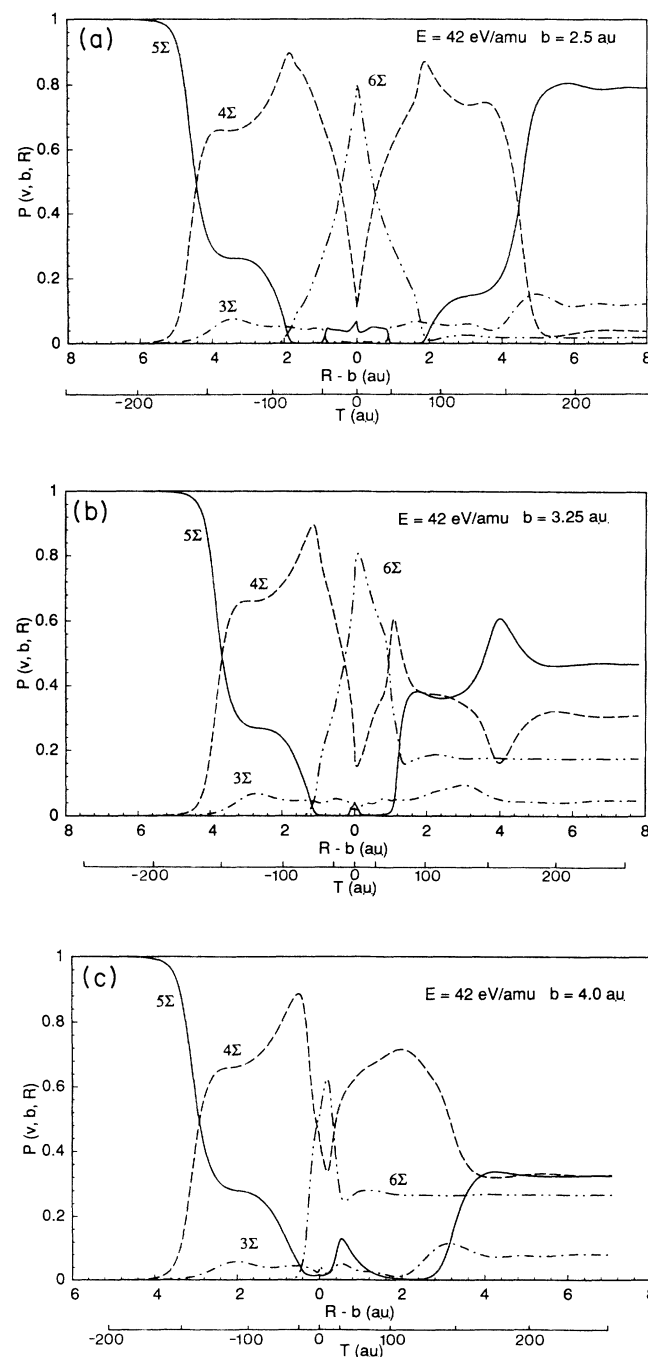


FIG. 9. Collision histories of transition probabilities as a function of R (and time) for the triplet system at (a) $b = 2.5$ a.u., (b) $b = 3.25$ a.u., and (c) $b = 4.0$ a.u. at $E = 42$ eV/amu.

probability for each state in the triplet and singlet systems at $E=42.0$ eV/amu in Figs. 8(a) and 8(b), respectively. The transition probabilities only to the $N^{3+}(2s3d)$, $N^{3+}(2s3p)$, and $N^{3+}(2p3s)$ states are dominant at this collision energy. In the triplet system, the $N^{3+}(2s3d)$ state mainly contributes to the total transition probability. The $N^{3+}(2p3s)$ state is also important; its contribution is larger than that from the $N^{3+}(2s3p)$ state at this energy. At lower energies, the contribution from

the $N^{3+}(2s3p)$ state steadily diminishes, but that from the $N^{3+}(2p3s)$ state is almost constant (see Fig. 3). The transition probability to the $N^{3+}(2p3s)$ state has the largest peak at an impact parameter nearly equal to R_3 and at impact parameters less than R_3 , the transition probabilities decrease with oscillation. This observation suggests that the transition to the $N^{3+}(2p3s)$ state occurs effectively only when the impact parameter is within the range of the avoided crossing R_3 . In the singlet system, the $N^{3+}(2s3d)$ state also contributes to the total transition probability most importantly. Although, at this collision energy, the contribution from the $N^{3+}(2s3p)$ state is comparable with that from the $N^{3+}(2p3s)$ state, at lower energies the contribution from the $N^{3+}(2s3p)$ state steadily diminishes, but that from the $N^{3+}(2p3s)$ state is almost constant (see Fig. 5). The transition to the $N^{3+}(2p3s)$ state starts at an impact parameter nearly equal to R_3 , but the rate of the decrease with decreasing impact parameter is weaker than in the triplet system.

Figures 9(a)–9(c) show the collision histories for the triplet system at $b=2.5$, 3.25, and 4.0 a.u., respectively, at $E=42.0$ eV/amu. These figures show that the transition to the 6Σ [$N^{3+}(2p3s)$] state is not from the 5Σ state but the 4Σ state. In the triplet system we have treated the avoided crossing at R_2 as diabatic, so the 4Σ and 5Σ states should be replaced by 5Σ and 4Σ states in the adiabatic sense at internuclear distances smaller than R_2 . At impact parameters much smaller than the avoided crossing R_3 , most of the flux of the 4Σ state transfers to the 6Σ state at the incoming part of the collision, but this transferred flux almost returns to the 4Σ state at the outgoing part of the collision. Thus, the transition probabilities of the $N^{3+}(2p3s)$ state are small. At impact parameters near R_3 , the transferred flux in the 6Σ state does not completely return to that of the 4Σ state. The remaining flux stays as the transition probability for the $N^{3+}(2p3s)$ state. The collision histories at $b=2.5$, 3.35, and 4.2 a.u. for the singlet system are shown in Figs. 10(a)–10(c), respectively, at $E=42.0$ eV/amu. Although at impact parameters smaller than the avoided crossing R_3 , the transition to the 8Σ [$N^{3+}(2p2s)$] state is from the 7Σ state, at impact parameters near R_3 , transfer from the 6Σ state also occurs. The collision histories for the singlet system are more complex than for the triplet system, in particular, at smaller impact parameters.

Although the contribution to the total cross section from the $N^{3+}(2p3s)$ state is small at the collision energies studied in this paper on the whole, at very low collision energies, below 10 eV/amu, this assumption may not be valid. The presence of the $N^{3+}(2p3s)$ state complicates the treatment of quantum-mechanical close-coupling calculations. A study of the effect of including this state is interesting and awaits a complete calculation in the future.

IV. SUMMARY OF CONCLUSIONS

Electron-capture cross sections have been obtained by applying semiclassical (12 and 13 channels for the triplet

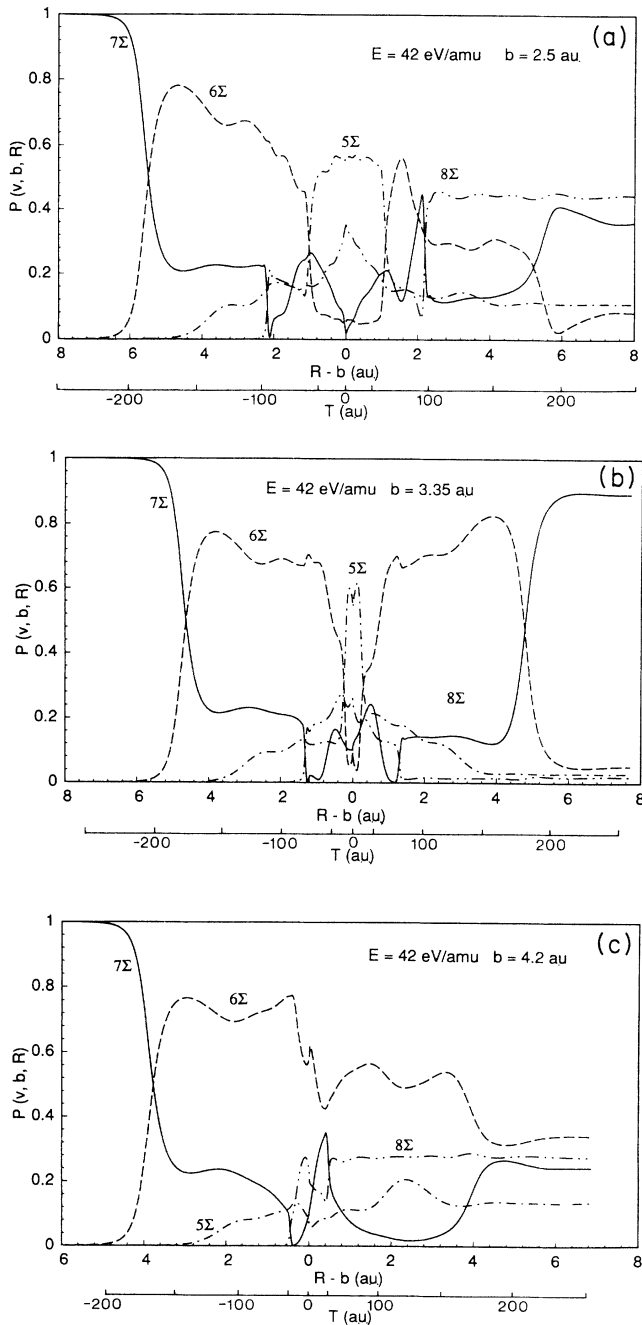


FIG. 10. Collision histories of transition probabilities for the singlet system at (a) $b=2.5$ a.u., (b) $b=3.35$ a.u., and (c) $b=4.2$ a.u. at $E=42$ eV/amu.

and singlet systems, respectively) and quantum-mechanical (two-channel) molecular orbital methods in the energy range from 1 eV/amu to 10 keV/amu. The results obtained are in good agreement with the measurements over the entire energy region studied. In the total cross sections, the oscillation appearing in the experiment is successfully reproduced in our calculation in the energy range 10–300 eV/amu and a theoretical rationale is provided. At low collision energies, the dominant state is $N^{3+}(2s3d)$ state. As the energy decreases, the total cross sections decrease. In the high-energy region, the dominant state is the $N^{3+}(2s3p)$ state, and the total cross sections gently decrease with collision energy. We have also included transfer-excitation processes such as the $N^{3+}(2p3s)$, $N^{3+}(2p^2)$, and $N^{3+}(2p3p)$ states. The most important state among all is the $N^{3+}(2p3s)$ state, but

even its contribution is not more than 10% of the total cross section.

ACKNOWLEDGMENTS

This work was supported in part by the U.S. Department of Energy, Office of Energy Research, Office of Health and Environmental Research, under Contract No. W-31-109-ENG-38 (M.K.); by the Office of Basic Energy Science, Division of Chemical Sciences, through Rice University (N.S.); and by the R. A. Welch Foundation (N.S.). N.S. was also supported by a Grant-in-Aid for Scientific Research from the Ministry of Education of Japan (01540312). Some portions of the present calculation were carried out at the computer centers of Tohoku University and Niigata University.

*Present address: Fujitsu Akita System Engineering Ltd., Akita, Japan.

- [1] See, for example, review articles on recent progress in the field. R. K. Janev, L. P. Presnyakov, and V. P. Shevelko, *Physics of Highly Charged Ions* (Springer-Verlag, Berlin, 1985).
- [2] N. Shimakura and M. Kimura, *Phys. Rev. A* **44**, 1659 (1991).
- [3] D. H. Crandall, R. A. Phaneuf, and F. W. Meyer, *Phys. Rev. A* **19**, 504 (1979).
- [4] W. E. Seim, A. Muller, I. Wirkner-Bott, and E. Salzborn, *J. Phys. B* **14**, 3475 (1981).
- [5] M. S. Huq, C. C. Havener, and R. A. Phaneuf, *Phys. Rev. A* **40**, 1811 (1989).
- [6] C. A. Feickert, R. J. Blint, G. T. Sturratt, and W. D. Watson, *Astrophys. J.* **286**, 371 (1984).
- [7] M. Kimura and N. F. Lane, in *Advances in Atomic, Molecular, and Optical Physics*, edited by D. R. Bates and B. Bederson (Academic, New York, 1989), Vol. 26, p. 79.
- [8] J. N. Bardsley, *Case Stud. At. Phys.* **4**, 299 (1974).
- [9] S. Bashkin and J. R. Stoner, Jr., *Atomic Energy Levels and Grotorian Diagrams I* (North-Holland, Amsterdam, 1975).
- [10] A. Dalgarno, *Adv. Phys.* **11**, 281 (1962).
- [11] H. Sato, M. Kimura, A. Wetmore, and R. E. Olson, *J. Phys. B* **16**, 3037 (1983).
- [12] M. Kimura, H. Sato, and R. E. Olson, *Phys. Rev. A* **28**, 2085 (1983).
- [13] T. G. Heil, S. E. Butler, and A. Dalgarno, *Phys. Rev. A* **23**, 1100 (1981).
- [14] B. R. Johnson, *J. Comput. Phys.* **13**, 445 (1973).
- [15] T. G. Heil and J. B. Sharma, *Phys. Rev. A* **36**, 3669 (1987).